5th Joint International Symposium on Deformation Monitoring (JISDM), 20-22 June 2022, Valencia, Spain
DOI: http://doi.org/10.4995/JISDM2022.2022.13417

A feasibility study for accelerated reference point determination using close range photogrammetry

Cornelia Eschelbach, Michael Lösler

Frankfurt University of Applied Sciences, Faculty 1: Architecture – Civil engineering – Geomatics, Laboratory for Industrial Metrology, Nibelungenplatz 1, 60318 Frankfurt am Main, Germany,
(cornelia.eschelbach@fb1.fra-uas.de; michael.loesler@fb1.fra-uas.de)

Key words: *reference point determination; close range photogrammetry; bundle adjustment; satellite laser ranging; GeoMetre*

ABSTRACT

The Global Geodetic Observing System (GGOS) aims for an accuracy of 1 mm in position concerning a global geodetic reference frame such as the International Terrestrial Reference Frame (ITRF). To derive a global frame, several space geodetic techniques are combined. The combination procedure requires the geometric relations between the invariant reference points of these techniques, the so-called local tie vectors. Each space geodetic technique defines its reference point individually, so the determination of the position of the reference point varies significantly between techniques. Within the international GeoMetre project, measurement systems and analysis strategies are developed to improve the quality of local tie vectors and, thus, the quality of the resulting global frame. The use of close range photogrammetry to determine the reference point of a telescope used for Satellite Laser Ranging (SLR) at the GGOS core station Wettzell in September 2020 is considered as a milestone in this project. This contribution deals with a novel approach for an accelerated reference point determination using close range photogrammetry. In comparison to the conventional photogrammetric approach, published so far, this new approach leads to a significant reduction in recording time. However, in case of inappropriate measurement configuration the approach also bears the risk of biased results. Most importantly, the new approach has the potential to be automated, which is one of the primary calls of GGOS for reference point determinations.

I. INTRODUCTION

One of the mayor challenges of humankind in this century is to face the global climate change. A reliable and high accurate geodetic infrastructure is essential for modelling the system Earth to get a better understanding of global processes. For instance, the detection of the rising of the sea-level requires accuracies of the reference frame of better than $0.5\ \mathrm{mm\,a^{-1}}$ in height position on a global scale. Four space geodetic techniques form a global frame of reference points, the International Terrestrial Reference Frame. Multi-technique stations host these space geodetic techniques close to each other on a single site and, therefore, play a key role in the combination process of the space geodetic techniques. These stations provide the so-called local ties: spatial vectors including the geometric relations between the invariant reference points of the techniques.

Local ties have been identified as a critical component within the combination process (Glaser *et al.*, 2015). Generating a local tie always consists of three determination steps: deriving the reference points of each space geodetic technique at a multi-technique station, combining the reference points in a consistent local reference frame including the related dispersion matrices, and, finally, transforming the local ties into the global reference frame (Lösler *et al.*, 2022). In total, GGOS aims for an accuracy of $1\ \mathrm{mm}$ for the reference points and, thus, also for the local ties.

The EURAMET project GeoMetre (2020) takes up the topic of improving the quality and reliability of global reference frames by, for instance, traceably transforming local ties to the global reference frame (Pollinger *et al.*, 2022). Also part of this research project is the further development of measurement and analysis strategies for the determination of the reference points of telescope-based space geodetic techniques. Two milestones have already been reached in this topic: a novel approach for the determination of reference points overcomes the necessity of synchronization between the measurement instrument and the telescope (Lösler *et al.*, 2018). Furthermore, close range photogrammetry has been applied to determine the reference point of an SLR telescope at the GGOS core station Wettzell (Figure 1) for the first time (Lösler *et al.*, 2021; 2022). During a measurement campaign in 2020, a first study proved the general suitability of close range photogrammetry for reference point determination. Nevertheless, the photogrammetric approach published so far is on the same level with standard methods in terms of handling and effort. This approach will be referred to as CRP approach (CRP: Close Range Photogrammetry) hereafter.

Figure 1. Satellite Observing System Wettzell at the GGOS core station Wettzell in the Bavarian Forest.

In this contribution, we present a novel photogrammetric measurement and analysis strategy, which is an advancement of the CRP approach. With this new approach, we mainly address the request to accelerate the measurement process and enable automation for data acquisition during regular telescope operation.

Section II describes the theoretical background and gives the most important formulas regarding the calculation algorithms of the bundle adjustment, the concatenated transformation and the determination of the reference point. In Section III, the measurement object and the circumstances for photogrammetry are mentioned. In addition, the measurement system and the measurement procedure are described in detail. The analysis strategy and the results are presented in Section IV. Finally, this contribution concludes with an outlook in Section V.

II. Theoretical background

The determination of the reference point of an SLR telescope in this approach consists of three analysis steps. The first step, described in Section II A, includes the determination of photogrammetric marker positions at the turnable part of the telescope structure in different telescope positions using a bundle adjustment. Section II B gives the formulas to reorient images using a concatenated transformation. This strategy enables the combination of data of a fixed object while the camera position is moved as well as with data of a fixed camera position while the object is moved. The camera positions chance during the measurement of the reference frame and of the telescope, which was oriented in eight different azimuth positions. On the other hand, fixed camera positions are used to measure the telescope in twelve further elevation positions per azimuth. Finally, in Section II C, the coordinates of all marker positions and their fully populated dispersion matrix serve as observations for the calculation of the reference point using the algorithms developed by Lösler *et al.* (2018). Due to the concatenated transformation, this approach is hereafter called the CRP-CT approach (CRP-CT: Close Range Photogrammetry using Concatenated Transformations).

A. *Bundle adjustment*

Each photogrammetric image provides the image coordinates of all visible marker positions. The image coordinates and the perspective center of the camera generate a spatial bundle of rays. Several ray bundles of several images taken from different perspectives form a stiff bundle network. The bundle adjustment orients all images and yields the interior and the exterior orientation parameters as well as the spatial coordinates of all marker positions, using the collinearity equations given by (Eq. 1):

$$\begin{pmatrix} x_i' \\ y_i' \end{pmatrix}_j = \begin{pmatrix} x_0' \\ y_0' \end{pmatrix} + \begin{pmatrix} x_i^* \\ y_i^* \end{pmatrix}_j + \begin{pmatrix} \Delta x_i' \\ \Delta y_i' \end{pmatrix}_j \tag{1}$$

with (Eqs. 2 and 3):

$$x_i^* = -c\frac{r_{11}(X_i - X_0') + r_{21}(Y_i - Y_0') + r_{31}(Z_i - Z_0')}{r_{13}(X_i - X_0') + r_{23}(Y_i - Y_0') + r_{33}(Z_i - Z_0')}, \tag{2}$$

$$y_i^* = -c\frac{r_{12}(X_i - X_0') + r_{22}(Y_i - Y_0') + r_{32}(Z_i - Z_0')}{r_{13}(X_i - X_0') + r_{23}(Y_i - Y_0') + r_{33}(Z_i - Z_0')}. \tag{3}$$

The equations serve as functional model for connecting the planar image coordinates $(x_i' \quad y_i')^{\mathrm{T}}$ with the corresponding spatial coordinates $(X_i \quad Y_i \quad Z_i)^{\mathrm{T}}$ of the photogrammetric targets. The principal distance c, the coordinates of the principal point $(x_0' \quad y_0')^{\mathrm{T}}$ and the distortion parameters $(\Delta x_i' \quad \Delta y_i')^{\mathrm{T}}$ are the parameters of the so-called interior orientation of the camera. The exterior orientation includes the spatial position $(X_0 \quad Y_0 \quad Z_0)_j^{\mathrm{T}}$ of the perspective centre and the rotation matrix $\mathbf{R}_j$, which reads (Eq. 4):

$$\mathbf{R} = \begin{pmatrix} r_{11} & r_{21} & r_{31} \\ r_{12} & r_{22} & r_{32} \\ r_{12} & r_{23} & r_{33} \end{pmatrix} \tag{4}$$

For the spatial orientation of the camera for each image. A detailed derivation of Equations 1-4 is given by, *e. g.*, Luhmann *et al.* (2019). Seven additional independent condition equations solve the datum defect of the estimation problem. The condition equations prevent any translation, rotation or scaling of the network by transforming the adjusted network to the approximation values of the datum points (Papo, 1982). Including these equations, a Gauß-Markov model can be set up. While the image coordinates serve as observations, the interior and the exterior orientation parameters as well as the spatial coordinates of the marker positions are parameters to be estimated (Förstner and Wrobel, 2016; Luhmann *et*

al., 2019). Since the parameters of the interior orientation are parameters to be estimated, this approach is known as self-calibration (Brown, 1971).

The estimated spatial coordinates of the photogrammetric markers are assigned for both the realization of a stable photogrammetric reference frame, which surrounds the measurement object, and deriving desired information about the measured object. Regarding the measurement campaign at Wettzell in 2020, the telescope was equipped with photogrammetric markers and rotated to different orientation positions. The spatial coordinates of the photogrammetric markers in different telescope positions were introduced to the calculation algorithm for the determination of the reference point of the SLR telescope (Lösler *et al.*, 2021; 2022).

During the measurement campaign further photogrammetric data were collected, which require an intermediate calculation step. In general, photogrammetric data acquisition means capturing images of an object from different positions providing as many different viewing angles as possible. Normally, the measured object remains fixed, and the camera is moved. But data acquisition also works inverted, i.e., when the camera is fixed and the measured object moves in front of the camera to take images from different viewing angles. Both strategies cannot be combined, if images contain subsets of moved and fixed photogrammetric markers. However, if, and only if, the moved marker subset is not related to the fixed reference frame via images, a contradiction-free combination by bundle adjustment is possible. Since the images of the moved object are unrelated to the fixed reference frame, the corresponding exterior orientation is determined only by the subset of photogrammetric markers at the moved object. In consequence of the unknown movement of the object, the camera is assumed to move in the opposite sense (Figure 2).

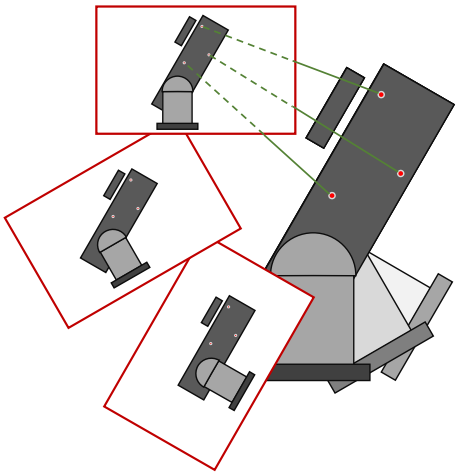

Figure 2. Estimated exterior orientations of subset images derived by the bundle adjustment; without image information concerning the fixed reference frame, the movement of an object, in this case the telescope, is interpreted as movement of the camera.

In order to provide correct spatial coordinates of the marker positions, the exterior orientations of these images, hereafter called subset images, have to be updated. In this approach, concatenated transformations relate the exterior orientations of the subset images to a reference exterior orientation referring to the fixed frame, which was obtained before the telescope rotated.

B. *Concatenated transformation*

The bundle adjustment yields the exterior orientation parameters of all images and the spatial coordinates of the photogrammetric markers. Subset images, which are exclusively oriented by a consistently moved subset of photogrammetric markers, are not yet properly oriented with respect to the fixed photogrammetric reference frame. The spatial coordinates of the marker positions provided by these images have to be transformed using the exterior orientation parameters of the reference image (Figure 3).

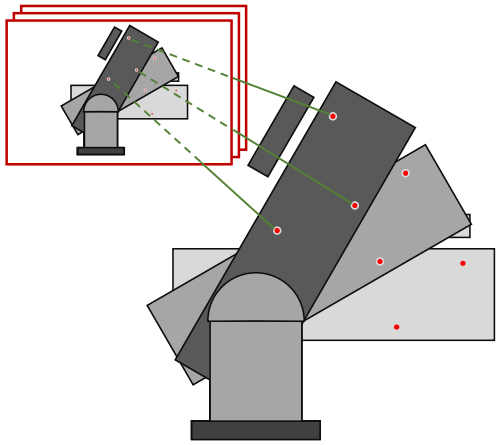

Figure 3. Re-oriented images after concatenated transformation; the rotation of the telescope is now apparent.

In fact, these exterior orientation parameters represent the true position and orientation of the camera at the time of the measurement. The set of exterior orientation parameters are combined to transform the spatial coordinates to the fixed photogrammetric reference frame. The concatenated transformation of the CRP-CT approach reads (Eq. 5):

$$\begin{pmatrix} X \\ Y \\ Z \end{pmatrix}_{\mathrm{Ref}} = \begin{pmatrix} X_0 \\ Y_0 \\ Z_0 \end{pmatrix}_{\mathrm{Ref}} + \mathbf{R}_{\mathrm{Ref}}^{\mathrm{T}} \mathbf{R}_{\mathrm{S}} \left[\begin{pmatrix} X \\ Y \\ Z \end{pmatrix}_{\mathrm{S}} - \begin{pmatrix} X_0 \\ Y_0 \\ Z_0 \end{pmatrix}_{\mathrm{S}} \right] \qquad (5)$$

Where $\mathrm{R}_{\mathrm{Ref}}$ is the rotation matrix orienting the reference image, R_{S} is the rotation matrix orienting the subset image. The translation vectors of the camera positions $(X_0 \quad Y_0 \quad Z_0)_{\mathrm{Ref}}^{\mathrm{T}}$ and $(X_0 \quad Y_0 \quad Z_0)_{\mathrm{S}}^{\mathrm{T}}$ belong to the reference image and to the subset image, respectively. The coordinates of an object point referring to the subset image are denoted by $(X \quad Y \quad Z)_{\mathrm{S}}^{\mathrm{T}}$, and $(X \quad Y \quad Z)_{\mathrm{Ref}}^{\mathrm{T}}$ is the corresponding

corrected position. Thus, the transformation provides the spatial coordinates of the marker positions related to the photogrammetric reference frame. By applying the propagation of uncertainty to Equation 5, the fully populated dispersion matrix is obtained for the transformed positions. These coordinates and their dispersion serve as input data for the determination of the reference point.

C. *Reference point determination*

The invariant reference point (IRP) of an SLR telescope is defined as the intersection of the azimuth axis and the elevation axis. If both axes do not intersect, the reference point is the point on the azimuth axis, which is nearest to the elevation axis. By definition, the IRP lies inaccessibly in the telescope structure and, therefore, can only be determined from targets, which are mounted at the telescope structure and measured in different telescope positions. Most commonly, polar measurement systems, *e. g.* total stations or laser trackers, provide the coordinates of the targets.

The simplest model for the calculation of biaxial telescopes like SLR or VLBI telescopes are spheres but this model is insensitive for any other telescope parameter except the position. Other approaches use circle models in different levels of complexity. When the telescope rotates around one axis while the other axis is fixed, targets at the turnable part of the telescope describe circles, which can be connected via several geometrical conditions (Eschelbach and Haas, 2003; Dawson *et al.*, 2007). Such models are rigorous but require dedicated telescope positions, and, thus, are unsuitable for a continuous reference point determination during regular telescope operations. The transformation model IRP-II presented by Lösler *et al.* (2018) overcomes the necessity of specific telescope positions, and provides the most complex set of telescope parameters.

The functional model of the IRP-II model reads (Eq. 6):

$$\mathbf{P}_{i,k} = \mathbf{P}_{\mathrm{IRP}} + \mathbf{R}_x(\beta)\mathbf{R}_y(\alpha)\mathbf{R}_z^{\mathrm{T}}(\kappa_k)\mathbf{R}_y(\gamma)1\mathbf{E} + \mathbf{R}_x(\omega_k)\mathbf{p}_i) \qquad (6)$$

And relates the point $\mathbf{p}_i^{\mathrm{T}} = (x_{\mathrm{i}} \quad y_{\mathrm{i}} \quad z_i)$ in a telescope fixed frame to its corresponding position $\mathbf{P}_{i,k}^{\mathrm{T}} = (X_{\mathrm{i}} \quad Y_{\mathrm{i}} \quad Z_i)$ in a fixed frame, *e. g.* the station network. The sub-indexed coordinate axes and the braced angles indicate the rotation axis and the rotation angle of the rotation matrices $\mathbf{R}$. Index k denotes the orientation of the telescope at the measurement time. The angles ω_k and κ_k are the azimuth angle and the elevation angle, respectively. The axis offset is considered by $\mathbf{E}^{\mathrm{T}} = (0 \quad e \quad 0)$. The tilt of the azimuth axis w.r.t. the Z-axis of the fixed frame is parametrized by the angles α, β, and γ is introduced to compensate for the deviation from the orthogonality of the two telescope axes. The translation vector $\mathbf{P}_{\mathrm{IRP}}$ is the invariant reference point.

The great advantage of IRP-II in contrast to former versions (Lösler, 2008), is that IRP-II overcomes the synchronization necessity between the measurement system and the telescope by introducing the rotation angles of the telescope as additional unknown parameters. Thereby the targets at the turnable part of the telescope can be measured during normal operations of the telescope. However, the application of the model depends on one condition: IRP-II requires at least two targets, which are observed at least partially at the same time. Photogrammetry fulfills this condition excellently, because images always contain several photogrammetric markers at the telescope. Therefore, the CRP approach as well as the CRP-CT approach presented in this contribution are suitable for data acquisition for IRP-II.

III. Measurement setup

A. *Satellite Observing System Wettzell*

The Geodetic Observatory Wettzell (GOW) is a GGOS core station and hosts all four space geodetic techniques. SLR telescopes measure the distances to satellites, which are equipped with retro reflectors. Therefore, an SLR telescope rotates around two axes, the azimuth axis and the elevation axis, to cover the sky. A rotatable protection dome encloses the telescope (*cf.* Figure 1). During a measurement campaign in 2020, close range photogrammetry was applied to determine the reference point of the SOS-W using the CRP approach for the first time. Further photogrammetric data was captured, the CRP approach was refined and integrated in an extended analysis procedure, which is presented for the first time and referred to as CRP-CT approach in this contribution.

B. *Measurement setup*

Hexagon's Aicon DPA Industrial measurement system is chosen for the data acquisition and pre-analysis. The photogrammetry system consists of the digital camera C1, a Canon EOS 5D, which is protected by a robust and extremely stiff IP51-rated camera case, and the analysis software Aicon Studio 3D. The maximum permissible error (MPE) of a measured length between two signalized points is specified by $15\ \mu\mathrm{m} + 15\ \mu\mathrm{m\ m}^{-1}$. The typical standard deviation of a position-based measurement obtained by a bundle adjustment is stated by $2\ \mu\mathrm{m} + 5\ \mu\mathrm{m\ m}^{-1}$ (Hexagon, 2019).

The DPA Industrial works with uncoded and coded circular black-and-white markers. About 225 14 bit coded markers at the dome wall and on the height level of the protecting dome establish the photogrammetric reference frame. Three certified scale bars, which are traced to the SI meter, provide the scale information for the photogrammetric reference frame, and contribute to all three coordinate components.

Furthermore, the dome wall is equipped with nine interoperable 1.5" drift nests, which magnetically support both reference markers for photogrammetric

systems and corner cube reflectors for multi-lateration coordinate measurement systems (Guillory *et al.*, 2020) and for polar measurement systems such as laser trackers or total stations (Lösler *et al.*, 2018). The interoperability facilitates the integration of the photogrammetric reference frame into the station survey network later on.

As in the CRP approach, the telescope is prepared with uncoded photogrammetric markers. The maximum distance between these markers and the elevation axis of the telescope is about $1\ \mathrm{m}$ and the markers cover an area of about $1\ \mathrm{m}^2$.

The CRP-CT approach works with additional coded markers on the telescope. Twelve coded markers are randomly attached between 14 uncoded markers (Figure 4). The coded markers at the telescope ensure a reliable orientation of the image while coded markers of the surrounding reference frame are covered and, therefore, are not captured.

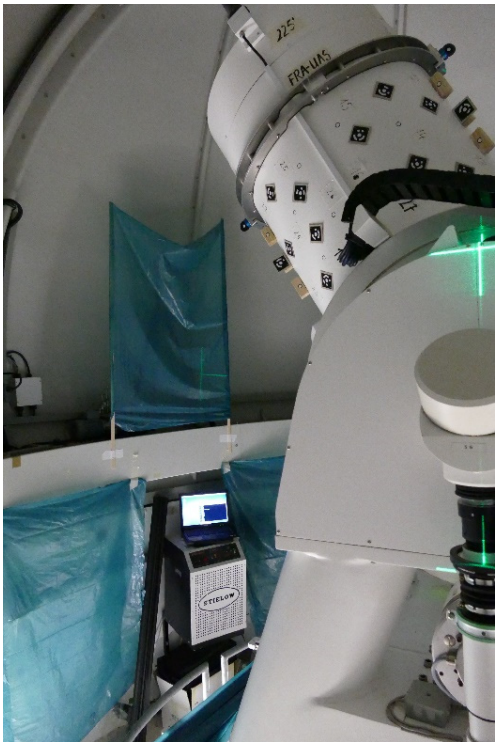

Figure 4. SLR-telescope prepared with coded and uncoded photogrammetric markers. The fixed photogrammetric reference frame in the background is covered with blue foil. The luminous green cross indicates the principal axis of the camera while the camera is fixed in the azimuthal reference position.

The telescope rotates to a specific azimuth and elevation position, which allows an excellent photogrammetric image capturing for the telescope markers in combination with the photogrammetric reference frame. The last image for this telescope position is captured from a fixed camera position, and is called the azimuthal reference image. For this camera position (Figure 5), as many telescope markers as possible have to remain visible, when the telescope rotates around the elevation axis.

Figure 5. Fixed camera position on a stable tripod for one of eight azimuthal reference positions. Photogrammetric reference points beyond the camera's field of view, for instance under the tripod, are not covered. Image acquisition is performed by remote control.

After capturing the azimuthal reference image, the photogrammetric reference frame behind the telescope is covered completely as shown in Figure 4. The telescope rotates stepwise to twelve elevation positions to cover the full range of motion of the axis, and the fixed camera captures one image per elevation position (Figure 4). Figures 4 and 5 show this scenario for elevation 225° from different perspectives. In absence of the reference frame in the background, the coded markers at the telescope exclusively define the exterior orientation of the image. From the perspective of the measurement process, the selection of the reference position of the telescope depends on two aspects: accessibility for photogrammetric measurements and a suitable position for the fixed camera. This study focuses on photogrammetric aspects; therefore, the azimuthal reference position is set to $90°$ elevation, which offers the widest configuration for image capturing.

To guarantee the stability of the camera position during all elevation positions referring to the azimuthal reference position, the camera is mounted on a stable tripod, and the images are captured via remote control. Once all elevation positions are measured, the cover of the photogrammetric reference frame is removed, and a new set of coded markers replaces the spent coded markers at the telescope. To avoid overlaps in the range of the point numbers, the removed coded markers must not be used again in the current experiment. The telescope rotates to the next azimuth position to continue the image capturing for the next azimuthal

reference position. In total, the telescope rotated to eight azimuth positions in combination with thirteen elevation positions in the CRP-CT approach.

Summarized, image capturing aims for three different aspects here:

1) For the determination of the photogrammetric reference frame, which is carried out at the beginning and at the end of an experiment.
2) For measuring different azimuth positions of the telescope, which will serve as azimuthal reference positions for the concatenated transformation.
3) For increasing the number of marker positions by further elevation positions, to cover the working range of the telescope.

The full configuration was performed independently twice, on day of year (DOY) 262 and 263 in 2020, respectively.

The effort of image capturing for the determination of the photogrammetric reference frame is identical in both the CRP and the CRP-CT approaches. The effort for acquiring the coordinates of the marker positions for different azimuth and elevation positions of the telescopes significantly differs in the two approaches. The conventional measurement of one telescope position requires approximately 20 images. For the CRP approach, all telescope positions consisting of up to six azimuth positions and seven elevation positions were measured conventionally. In the CRP-CT approach, only one elevation positon per azimuth was measured conventionally, while twelve further elevation positions per azimuth were captured by one image each. The CRP-CT approach reduced the required time to less than a tenth compared to the CRP approach. Nevertheless, the time to cover the photogrammetric reference frame narrows the benefit depending on the concept of handling. For the purpose of a feasibility study, lightweight semi-transparent foil and wooden struts were sufficient (Figure 4). In total, the strategy of the CRP-CT approach at least halved the time effort for the data acquisition compared to the CRP approach or approaches using polar measurement systems with a comparable number of telescope positions.

IV. Analysis and results

The Aicon DPA Industrial measurement system includes the software package Aicon Studio 3D for storage management of the images, automated measurement of the image coordinates and pre-analysis to evaluate the quality and usability of the images. The bundle adjustment follows the procedure described in Section II A. The adjustment is based on the approximation values of the pre-analysis and provides the parameters of the interior orientation of the camera, the exterior orientations of the images, and the spatial coordinates of the photogrammetric markers. The datum refers to the nine markers defined by the positions of the drift nests. Since only the standard deviations of the spatial coordinates are provided by the commercial software, the bundle adjustment was implemented in the in-house software JAiCov (2021). JAiCov reprocesses the final result from Aicon Studio 3D to obtain the fully populated dispersion matrix.

Lösler *et al.* (2021; 2022) studied the potential of close range photogrammetry for the reference point determination of an SLR telescope and presented the results of seven independent experiments applying the CRP approach at DOY 255-260 and 264 in 2020. The measurements for the CRP-CT approach were carried out in the same period at DOY 262 and 263. For the CRP-CT approach the mean standard deviations of the coordinate components of the marker positions in different telescope orientations are in the range of $0.01\ \mathrm{mm}$ to $0.02\ \mathrm{mm}$. The values given in Table 1 are slightly smaller in comparison to the results of the experiments presented by Lösler *et al.* (2021). The reason can be found in the subset images, which participate in the solution of the bundle adjustment and refine the coordinates of the marker positions. Although they do not directly contribute to the determination of the absolute marker positions, they strengthen the geometric connection.

Table 1. Benchmark data of bundle adjustment of experiment days 262 and 263 in comparison with results for days 255, 256 and 264 given by Lösler *et al.* (2021): n_{obs} and n_{par} are the number of observations and unknowns, respectively. The mean standard deviations of the marker positions are $\bar{\sigma}_X$, $\bar{\sigma}_Y$, $\bar{\sigma}_Z$ and $\bar{\sigma}_{3D}$. Standard deviations are given in mm.

DOY	n_{obs}	n_{par}	$\bar{\sigma}_X$	$\bar{\sigma}_Y$	$\bar{\sigma}_Z$	$\bar{\sigma}_{3D}$
255	64 367	10 015	0.03	0.03	0.02	0.05
256	82 905	13 003	0.03	0.03	0.02	0.05
262	36 763	4 828	0.02	0.02	0.01	0.03
263	44 299	5 572	0.01	0.01	0.01	0.02
264	120 005	13 663	0.02	0.02	0.01	0.03

The spatial coordinates of 112 marker positons, which belong to the eight azimuthal reference positions, were immediately used for the determination of the reference point. The marker positions derived by the subset images in different telescope positions had to be transformed to the photogrammetric reference frame using the formulas presented in Section II B. The number of transformed marker positions is 1268 at DOY 262 and 1282 at DOY 263, and does not meet the theoretical value 1344 resulting from eight azimuth and thirteen elevation positions. A small number of marker positions is missing because they were obscured by parts of the telescope structure during image acquisition or could not be measured due to a poor viewing angle. In total, for a single CRP-CT experiment 1380 and 1394 marker positions and their fully populated dispersion matrix were introduced to the reference point determination of DOY 262 and 263, respectively. For comparison, the CRP approaches of

DOY 264 provided 588 marker positions from six azimuth positions and seven elevation positions with the same number of markers at the telescope.

The calculation of the reference point of the SLR telescope followed the IRP-II model developed by Lösler *et al.* (2018) and presented in Section II C. Figure 6 depicts the results for the invariant reference point $\mathbf{P}_{\mathrm{IRP}}$ derived by the different photogrammetric approaches. The solutions of DOY 255 to 260 and 264 are taken from Lösler *et al.* (2022).

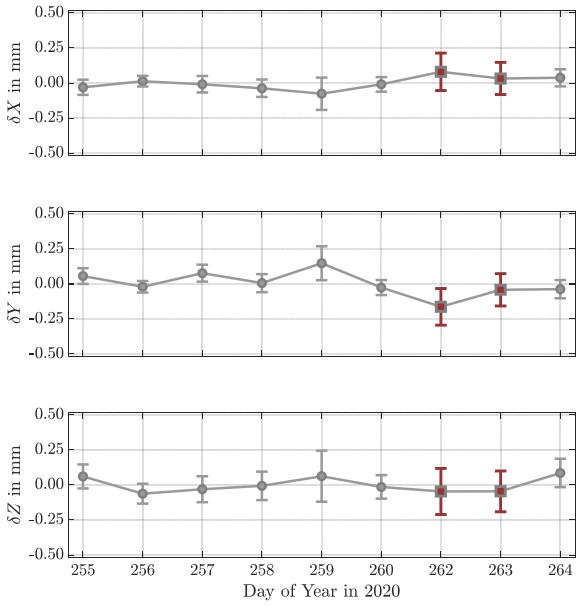

Figure 6. Results for the invariant reference point including 3σ error bars derived by different photogrammetric approaches. The results of DOY 262 and 263 refer to the CRP-CT approach and are denoted by red squares. The results of the CRP approach are denoted by grey circle and were derived by Lösler *et al.* (2022).

The solutions of DOY 262 and 263 refer to the CRP-CT approach. They fit very well into the sequence of solutions derived by the CRP approach. The position of the reference point for nine individual experiments varies in the X-component by $0.16\,\mathrm{mm}$, in the Y-component by $0.31\,\mathrm{mm}$, and in the Z-component by $0.15\,\mathrm{mm}$. The 3σ confidence interval for the X-component and Y-component does not exceed $0.12\,\mathrm{mm}$ and $0.20\,\mathrm{mm}$, respectively. The 3σ confidence interval for the Z-component is the largest of the three components and amounts to $0.33\,\mathrm{mm}$. The reason can be found in the measurement configuration for the uncoded markers at the telescope related to the surrounding reference frame. While the photogrammetric markers of the reference frame enclosed the reference point in the horizontal component, the height of the reference frame did not include all measured marker positions.

Even though the results of this photogrammetric approach fit very well into the results of the complete measurement campaign, the question of biased results in case of unfavorable recording configurations cannot be answered conclusively. A risk for biased results lies in an unfavorable choice of the telescope's reference position, to which all elevation positions for this azimuth are related by the concatenated transformation. The configuration used in this approach does not have a noticeable negative effect on the results, especially not on the position of the reference point.

V. Conclusion and Outlook

Improving the quality and reliability of local tie vectors is one of the major tasks in the EURAMET project GeoMetre. GGOS calls for an accuracy of $1\,\mathrm{mm}$ for the local ties, including the reference point determination of each space geodetic technique, the combination of the reference points in a consistent local reference frame, and the transformation of the local ties into the global reference frame. As many components as possible should have a high potential of automation in order to improve the acceptance of the application at multi-technique stations all over the world. Lösler *et al.* (2021; 2022) published promising results on the use of close range photogrammetry to determine the reference point at the SOS-W in Wettzell. This paper presented a modified method for using close range photogrammetry, which significantly reduces the measurement time. In this feasibility study, the measurement time was halved, while doubling the measured telescope positions. The accuracy of the position of the reference point was comparable to results derived from the observation material of polar measuring systems (Eschelbach and Haas, 2003; Lösler *et al.* 2018).

The use of close range photogrammetry also has the potential for automation. In the CRP-CT approach, the transformation parameters for the concatenated transformation were entirely obtained from the photogrammetric data. Modern total stations are equipped with on-board cameras, which provide images for a visual impression of the environment of the measurement object. The quality of the images does not yet reach the quality of a photogrammetric camera. However, first investigations to use these built-in cameras as measuring sensor show promising results (Schestauer *et al.* 2017). The combination of a total station with a high-quality built-in camera will be able to combine the advantages of polar observations and photogrammetric observations. The parameters of the exterior orientation of an image may then result from the orientation of the total station. The simultaneous measurement of polar observations to reflectors at the telescope will improve the stability of the algorithm. The number of photogrammetric markers is not relevant for the measurement time, and the measurement of a single reflector by a total station only costs seconds. Such a fast measurement configuration is suitable to eliminate the down times for surveying the reference point of VLBI and SLR telescopes during their regular operations. The application of the novel

approach presented in this contribution in combination with upcoming technological developments will reduce measurement times and effort for the reference point determination, leading to an increased deployment at multi-technique stations.

VI. Availability of data and material

All data analyzed in this investigation are available online. The data sets of the common CRP approach, *i.e.,* DOY 255-260 as well as 264, are available online at https://doi.org/10.3390/app11062785. The data sets of the novel CRP-CT approach, *i.e.,* DOY 262 and 263, are available at https://doi.org/10.5281/zenodo.6482984.

VII. Acknowledgements

We thank Swetlane Mähler and Dr. Stefan Riepl from the Geodetic Observatory Wettzell for their support during the fieldwork. This project 18SIB01 GeoMetre has received funding from the EMPIR programme co-financed by the Participating States and from the European Union's Horizon 2020 research and innovation programme.

References

Brown, D.C. (1971). Close-Range Camera Calibration. *Photogrammetric Engineering*, 37, pp. 855–866.

Dawson, J., P. Sarti, G. M. Johnston, and L. Vittuari (2007). Indirect approach to invariant point determination for SLR and VLBI systems: an assessment. *Journal of Geodesy*, 81(6-8), pp. 433–441. DOI: 10.1007/s00190-006-0125-x

Eschelbach, C., and R. Haas (2003). The IVS-reference point at Onsala – high end solution for a real 3D-determination. In *Proceedings of the 16th Working Meeting on European VLBI for Geodesy and Astrometry*, Schwegmann, W., and Thorandt, V., Eds.; Bundesamt für Kartographie und Geodäsie, pp. 109–118.

Förstner, W., and B.P. Wrobel (2016). Photogrammetric Computer Vision—Statistics, Geometry, Orientation and Reconstruction; *Geometry and Computing*, 11; Springer. DOI: 10.1007/978-3-319-11550-4

GeoMetre (2020). *Large-Scale Dimensional Measurements for Geodesy - A Joint Research Project within the European Metrology Research Programme EMPIR*; European Commission (EC), Grant Number: 18SIB01; EURAMET e.V.: Brunswick, Germany. DOI: 10.13039/100014132

Glaser, S., M. Fritsche, K. Sośnica, C.J. Rodríguez-Solano, K. Wang, R. Dach, U. Hugentobler, M. Rothacher, and R. Dietrich (2015). Validation of Components of Local Ties. In *REFAG 2014*; van Dam, T., Ed.; Springer; Vol. 146, pp. 21–28. DOI: 10.1007/1345_2015_190

Guillory, J., D. Truong, and J.-P. Wallerand (2020). Uncertainty assessment of a prototype of multilateration coordinate measurement system. *Precision Engineering*. DOI: 10.1016/j.precisioneng.2020.08.002

Hexagon (2019). AICON DPA Series—Unrivalled High-End Photogrammetry Systems, Datasheet; Hexagon Manufacturing Intelligence: Shenzhen, China. Available online: https://hexagonmi.com (accessed on 22 December 2021)

JAiCov (2021). Java Aicon Covariance matrix—Bundle Adjustment for Close-Range Photogrammetry. Available online: https://github.com/applied-geodesy/bundle-adjustment (accessed on 15 December 2021).

Luhmann, T., S. Robson, S. Kyle, and J. Boehm (2019). *Close-Range Photogrammetry and 3D Imaging*, 3rd ed.; de Gruyter: Berlin, Germany. DOI: 10.1515/9783110607253

Lösler, M. (2008). Reference point determination with a new mathematical model at the 20 m VLBI radio telescope in Wettzell. *Journal of Applied Geodesy*, 2(4), pp. 233–238. DOI: 10.1515/JAG.2008.026

Lösler, M., C. Eschelbach, and T. Klügel (2022). Close Range Photogrammetry for High-Precision Reference Point Determination: A Proof of Concept at Satellite Observing System Wettzell. In *Proceedings of the 2021 IAG Symposium*; Freymueller, J.T. and Sánchez, L., Eds.; Springer. DOI: 10.1007/1345_2022_141

Lösler, M., C. Eschelbach, T. Klügel, and S. Riepl (2021). ILRS Reference Point Determination using Close Range Photogrammetry. *Applied Sciences*, 11(6), 2785, 2021. DOI: 10.3390/app11062785

Lösler, M., C. Eschelbach, and S. Riepl (2018). A Modified Approach for Automated Reference Point Determination of SLR and VLBI Telescopes. *Technisches Messen*, 85(10), pp. 616–626. DOI: 10.1515/teme-2018-0053

Papo, H.B (1982). Free Net Analysis in Close-Range Photogrammetry. *Photogrammetric Engineering and Remote Sensing*, 48(4), pp. 571–576.

Pollinger, F., S. Baselga, C. Courde, C. Eschelbach, L. García-Asenjo, P. Garrigues, J. Guillory, P. O. Hedekvist, T. Helojärvi, U. Kallio, T. Klügel, P Köchert, M. Lösler, R. Luján, T. Meyer, P. Neyezhmakov, D. Pesce, M. Pisani, M. Poutanen, G. Prellinger, A. Röse, J. Seppä, D. Truong, R. Underwood, K. Wezka, J.-P. Wallerand, and M. Wiśniewski (2022). The European GeoMetre project – developing enhanced large-scale dimensional metrology for geodesy. *5th Joint International Symposium on Deformation Monitoring* (JISDM), 20-22 June 2022, Valencia, Spain.

Schestauer, B.-J., A. Wagner, W. Wiedemann, and T. Wunderlich (2017). Tachymetrisches 6DOF-Messverfahren. In Ingenieurvermessung 17: Beiträge zum 18. *Internationalen Ingenieurvermessungskurs Graz*; Lienhart, W., Ed.; Wichmann: Offenbach, Germany, pp. 213-220.